

The formation and differentiation of magmas

Bortnikov N.S.¹, Kryazhev S.G.², Gorelikova N.V.¹, Smirnov S.Z.³, Gonevchuk V.G.⁴, Semenyak B.I.⁴, Dubinina E.O.¹, Sokolova E.N.³ The fluid regime of Badzhals hydrothermal-magmatic system of the Far East (Priamurie, Russia).

¹Institute of ore deposits, petrography, mineralogy and geochemistry RAS, Moscow, (bns@igem.ru, ngor@igem.ru); ² Central Geological Research Institute for Nonferrous and Precious Metals, Moscow, (S34@mail.ru); ³Institute of geology and mineralogy after V.S.Sobolev of Siberian Division RAS, Novosibirsk, (ssmr@igm.nsc.ru); ⁴Far East Geological Institute RAS, Vladivostok.

Abstract. The Badzhals tin district in the western part of Khabarovsk krai is a part of the Khingans–Okhotsk metallogenic province. The most important Pravourmiisky greisen deposit is unique because contains 3.8% of Russia's total tin reserves. The small and medium Blizhnee, Boltoro, Dvoinoe, Loshadinaya Griva, Rudnoe, and Omot–Makit deposits are known in the Badzhals tin district. The Blizhnee medium deposit has been partly abandoned by prospectors.

The evolution of the Badzhals tin magmatic–fluid system of the eponymous volcanoplutonic zone in the Middle Amur Region has been studied to reveal special characteristics of the transition from granite crystallization to rare metal deposition. Therefore, the authors have conducted an in-depth study of melt, fluid–melt, and fluid inclusions and oxygen isotope composition of minerals from granitic rocks of the Verkhneurmiisky pluton within the Badzhals volcanoplutonic zone and minerals of the Pravourmiisky and Blizhnee Sn–W deposits. Greisen alteration and hydrothermal veins at the Pravourmiisky and Blizhnee deposits resulted from a single magmatic–fluid system related to the Verkhneurmiisky granite pluton, which is one of the domes of the Badzhals batholith.

The great significance of volatile components such as F, Cl and H₂O has been revealed under the granite crystallization and generation mineral-forming fluid from the early magmatic stage to the late hydrothermal one. The Cl and F concentrations in glasses are 0.03–0.14 and 0.14–0.44 wt %, respectively, and are higher than those in the bulk rock compositions, 0.02 and 0.05–0.13 wt %, respectively. These differences indicate that Cl and F could have been removed from a granitic melt during its crystallization and degassing. The H₂O concentration estimated based on the electron deficiency of summed microprobe analyses is 8–10 wt %. This was estimated taking into account the possible effect of "sodium loss" (Nielsen and Sigurdson, 1981) when analyzing hydrated glasses. Taking into account the high uncertainty of such estimation (Devine et al., 1995), this value is extremely uncertain and the studied melts should be considered as containing 9.5–10.0 wt % H₂O. The agreement between the measured data and those calculated based on the suggested model indicates that a significant volume of external fluid having different isotopic features and not in equilibrium with the Verkhneurmiisky granite did not enter the magmatic–fluid system. The revealed differences in the physicochemical formation conditions of the two studied deposits are not critical and

support their formation within a single magmatic–fluid system.

Keywords: Badzhals district, tin–tungsten deposits, granites, greisens, magmatic–hydrothermal system, transition stage, melt inclusions, thermobarogeochemistry, vapour separating, fluid evolution, H₂O, Cl, F, oxygen isotopes.

Tin–tungsten deposits. The genetic relation of Sn and Sn–W ores to granites is based not only on their spatial association with intrusions, but on geochronological data as well. The latter indicate the close crystallization of magmatic rocks and ore deposition (Darbyshire and Shepherd, 1985).

In particular, the time gap between granite crystallization and ore deposition is no longer than a few million years (Lehman, 1990). To explain these controversial issues, we have studied two deposits from the Badzhals tin-bearing greisens magmatic–fluid system. These are the Pravourmiisky (greisen) related to the contact of the Verkhneurmiisky pluton, whose rocks have features of both I- and S-type granites (Gonevchuk, 2002) and the Blizhnee, which is located approximately 50 km NE of Pravourmiisky and related to granitic stock similar in composition to the granites of the pluton. Therefore, we have examined melt and fluid inclusions in quartz, the oxygen isotope composition of quartz from phenocrysts in granite and porphyry granite, and fluid inclusions and the oxygen isotope composition of quartz, topaz, and cassiterite from orebodies.

Results. Melt inclusions have been examined in quartz from six samples of Verkhneurmiisky granite and porphyry granite. These rocks are peraluminous (Table 1): $A/CNK = Al_2O_3/(CaO + Na_2O + K_2O) = 0.98–1.1 \geq 1.0$, although their compositions are close to the boundary between per- and metaluminous granites, $A/CNK = 1$ (Maniar and Piccoli, 1989). They are attributed to the calc–alkaline series in their $K_2O + Na_2O - CaO$ coefficient, 5.62–7.64. Rubidium, Y, Pb, Zn, Sr, Nb, Ba, Zr, Sn, Cr, V, Ni, and Co were detected in them (Table 1). These rocks are enriched in some large-ion lithophile elements (LILE), such as Rb, Pb, and K, and are depleted in Nb and Zr, which belong to the high-field-strength elements (HFSE). Thirteen melt inclusions 10 to 20 μm in size were examined. They are completely filled with an aggregate of daughter crystalline phases at room temperature. The small size of most inclusions (below 10 μm) prevented reliable identification of the daughter phases. Fluid segregation similar to a deformed gas bubble is occasionally observed in them. Sample heating showed that quartz contain *normal* and *combined* melt inclusions. Inclusions in which both silicate melt and aqueous solution are trapped pertain to the

latter. Melt inclusions are observed one by one and less frequently form groups of several inclusions. This is an obvious indication that inclusions are primary (Roedder, 1984) and were trapped during crystallization of host mineral. This indicated their simultaneous entrapment in quartz. Both melt and fluid inclusions are present in the same group.

Analyses were carried out at the Analytical Center of the Far East Geological Institute, Far East Branch, Russian Academy of Sciences. Contents of

Table 1. Description, composition, and normative component content of granites and porphyry granites of Verkhnemurmiisky pluton and Pravourmiisky dike.

Sample no.	BG-21	BG-23	BG-25	BG-82	BG-104	BG-105	BG-48
SiO ₂	76.78	73.69	73.47	73.44	76.30	76.35	76.56
TiO ₂	0.05	0.17	0.20	0.19	0.06	0.10	0.14
Al ₂ O ₃	12.06	13.60	13.78	13.85	13.92	13.09	12.14
Fe ₂ O ₃	0.75	0.69	0.54	0.28	0.33	0.26	0.32
FeO	0.42	1.20	0.89	1.66	0.36	1.03	0.77
MnO	0.03	0.03	0.04	0.01	0.01	0.01	0.03
MgO	0.30	0.35	0.24	0.90	0.06	0.20	0.17
CaO	1.02	1.81	1.67	1.42	0.50	0.5	1.72
Na ₂ O	3.20	3.83	2.96	3.45	3.36	3.38	3.03
K ₂ O	4.62	4.28	5.23	4.01	4.78	4.58	4.31
Fire loss	0.47	0.11	0.69	0.21	0.15	0.37	0.63
H ₂ O [*]	0.05	0.02	0.15	0.04	0.13	0.00	0.00
P ₂ O ₅	0.14		0.16		0.03		0.09
F	0.12	0.20	0.10	0.17	0.13	0.05	0.07
Total	99.96	99.96	99.97	99.59	99.99	99.92	99.98
Rb	580	199	210	180	200	245	
Sr	16	62	84	100	45	40	
Ba	33		450	478	345	308	
Zr		93	95	111	621	90	
Nb	48	17	32	13	17	18	
Y	110	29	63	29	73	47	
Ni	-	9	5	8	-	-	
Co	-	5	3	-	-	-	
Cr	-	19	16	19	-	-	
V	3	52	28	48	5	17	
Cu	15	37	18	46	6	13	
Sn	5	4	3	5	4	7	
Pb	33	45	35	23	34	24	
Zn	-	65	76	58	44	62	
Na ₂ O+K ₂ O	7,82	8,11	8,19	7,46	8,14	7,96	7,34
K ₂ O/Na ₂ O	1,44	1,12	1,77	1,16	1,42	1,36	1,42
A/CNK	1,05	1,05	0,98	1,10	1,10	1,10	0,95
Fe/Fe+Mg	0,87	0,94	0,95	0,70	0,70	0,93	0,88
Ab	27,34	32,44	25,10	29,43	28,50	28,73	25,75
Q	38,12	29,75	31,25	32,44	36,89	37,02	38,60
Or	27,58	25,32	30,98	23,90	28,32	27,20	25,58

oxides and F were determined with bulk chemical analysis and atomic absorption spectrometry, respectively; analysts L.A. Avdenina, S.P. Batalova, and G.I. Makarova. Trace element concentration was measured using inductively coupled plasma mass spectrometry; analysts M.G. Blokhin and D.S. Ostapenko. Contents of normative components normalized to 100% are given. LOI, loss of ignition; n.a., element not analyzed; b.d.l., content of element is below detection limit; Ab, albite; Q, quartz; Or, orthoclase. BG-23, near-contact pseudoporphyratic biotite apatite-bearing granite. BG-25, pseudoporphyratic biotite apatite-bearing granite at the contact with rhyolite. BG-82, chloritized pseudoporphyratic biotite granite with accessory allanite, xenotime, and monazite. BG-104 and BG-105, holocrystalline medium-grained biotite granite with accessory zircon and monazite. BG-48, chloritized porphyry granite (porphyry rhyolite). BG-21, fine-grained biotite (with muscovite and fluorite) granite from stock in near-contact pseudoporphyratic biotite granite (Table 1).

Glass Composition in Melt Inclusions.

The glass composition in inclusions varies significantly (Table 2): all of them are felsic (69.1–73.2 wt % SiO₂) and corresponds to felsite melt (Le Maitre et al., 2002). Total alkali ranges from 6 to 9 wt %. The alumina saturation index (A/CNK) in glasses ranges from 0.95 to 1.33 (Fig. 4). Low A/CNK index in glasses was identified in inclusions from quartz in samples BG-25, 82, and 104. This index is variable not only from one sample to another, but in the single sample. The A/CNK value (0.98–1.15) in glasses from inclusions in sample BG-21 is close to the boundary between per- and metaluminous granites (Fig. 4), whereas glasses from samples BG-23 and 105 are peraluminous (A/CNK 1.1–1.33). Rare alkalis Rb₂O and Cs₂O were detected in glasses (Table 2).

Based on the study of melt and fluid inclusions in quartz of granites the contents of fluid components in melt and in rocks were determined by calculation method, as well as the composition of magmatic fluid in equilibrium with the melt and the composition of the magmatic fluid after the complete crystallization of the granite (Table 3).

L. Ya. Aranovich modeled the evolution of the Badzhal hydrothermal-magmatic system and calculated the parameters of the system and the content of volatiles at different stages of its development.

Volatiles: chlorine and fluorine. The Cl and F concentrations in glasses are much

The formation and differentiation of magmas

higher than those in rocks (Tables 1, 2), which is apparently associated with separation of chlorine and, to a lesser extent, fluorine from the granite melt during its crystallization and related degassing. The F content in glasses is much lower than that in melts from inclusions in Li–F granites (Kovalenko, 1977); granite pegmatites enriched in Br, F, and rare metals (Smirnov, 2015); and Zinnwald tin-bearing microgranites, 4.9 ± 0.3 wt % (Thomas and Klemm, 1997). The Cl content is comparable with that from melt inclusions in quartz from rocks of Bolivian porphyry tin systems (~ 0.13 – 0.22 wt %), whereas the F concentration (≤ 0.15 wt %) is higher.

Water. The H₂O content in melt was estimated from the electron deficiency in the summed

microprobe analyses inclusions. The possible effect of sodium loss was taken into account (Nielsen and Sigurdson, 1981). Such estimation depends on the accuracy in determining the major constituents in glasses, but it allows estimation of the volatile content compared to that obtained from independent measurements (Thomas and Klemm, 1997) therefore, it is widely used in practice (e.g., Aranovich et al., 2013). The estimated H₂O concentration in glasses ranges from 3.8 to 11.5 wt % (Table 2). It is higher in glasses richest in Al. (Dietrich et al., 2000). The bulk F content in rocks of those systems was also low, 0.07–0.27 wt %.

Table 2. Electron microprobe data for glasses from melt inclusions in quartz of granites and estimated water content.

Sample no					BG-23		BG-25		BG-82	BG-104	BG-105		
	1	4	6	7	1	3	2	4	1	5	6	5	2
SiO₂	69.14	70.31	69.99	70.68	71.6	72.75	72.74	69.23	73.18	70.34	71.12	70.4	71.36
TiO₂	n.d.	0.09	0.04	0.01	0.1	0.01	0.01	0.02	n.d.	n.d.	0.07	n.d.	0.03
Al₂O₃	12.87	11.75	12.18	10.73	12.12	10.71	11.94	13.7	12.75	10.16	11.2	11.41	11.47
FeO	0.48	1.02	0.54	0.59	0.72	0.46	0.18	0.23	0.28	0.21	0.31	0.29	0.11
CaO	0.13	0.12	0.15	0.13	0.03	0.2	0.24	0.59	0.21	0.24	0.27	0.3	0.26
Na₂O	5.26	3.58	4.66	3.46	3	3.23	4.66	5	5.34	2.98	2.77	3.69	2.89
K₂O	3.92	3.77	3.68	3.36	3.78	3.65	3.22	3.99	3.86	4.26	3.25	3.44	3.45
Rb₂O	0.12	0.12	0.2	0.02	n.d.	0.08	0.1	0.01	n.d.	0.07	0.1	0.1	0.07
Cs₂O	0.14	0.1	0.09	0.17	0.1	0.08	n.d.	0.1	0.05	0.03	n.d.	0.04	n.d.
P₂O₅	n.d.	0.05	n.d.	0.02	0.05	n.d.	0.02	n.d.	0.02	n.d.	0.05	n.d.	n.d.
Cl	0.11	0.16	0.09	0.07	n.d.	0.06	0.11	0.14	0.14	0.09	0.09	0.2	0.09
F	0.4	0.43	0.37	0.42	0.15	0.44	0.47	0.28	0.33	0.14	0.25	0.28	0.31
Total	92.57	91.50	91.99	89.66	91.65	91.67	93.69	93.29	96.16	88.52	89.48	90.15	90.04
H₂O calc.	7.43	8.50	8.01	10.34	8.35	8.33	6.31	6.71	3.84	11.48	10.52	9.85	9.96

H₂O is estimated from electron deficiency of summed microprobe analyses.

Table 3. Calculation of the composition of magmatic fluid released during crystallization of granites of the Verkhneurmiiskiy massif.

Sample	BG-21	BG-23	BG-25	BG-82	BG-104	BG-105
Content of fluid components in melt, wt. %						
Cl	0.11	0.06	0.13	0.14	0.09	0.13
F	0.41	0.44	0.38	0.33	0.14	0.28
H ₂ O	8.57	8.33	6.51	3.84	11.48	10.11
Content of fluid components in rock, wt. % (Table 1)						
Cl*	0.02	0.02	0.02	0.02	0.02	0.02
F	0.12	0.20	0.10	0.17	0.13	0.05
H ₂ O	0.42	0.09	0.54	0.17	0.02	0.37
Composition of magmatic fluid in equilibrium with the melt, **wt. %						
Cl ⁻	2.20	1.20	2.60	2.80	1.80	2.60
F ⁻	0.08	0.09	0.08	0.07	0.03	0.06
NaCl+KF	3.90	2.26	4.55	4.85	3.07	4.49
Cl/F	26.83	13.64	34.21	42.42	64.29	46.43
The composition of the magmatic fluid after the complete crystallization of the granite, wt. %						
Cl ⁻	1.07	0.49	1.84	3.27	0.61	1.10
F ⁻	3.50	2.91	4.69	4.36	0.09	2.36
NaCl+KF	12.45	9.69	17.40	18.72	1.28	9.02
Cl/F	0.31	0.17	0.39	0.75	6.78	0.47

Table 4. Isotope abundance of oxygen of minerals and calculated values $\delta^{18}\text{O}$ aqueous phase in equilibrium fluid

Sample no	Mineral	$\delta^{18}\text{O}$ ‰ (mineral)	T, °C	$\delta^{18}\text{O}$ ‰ (fl)
<i>Granites of Urmi massif</i>				
BG-82	Quartz	11.2	580**	9.2 (q)
	Orthoclase	9.9		
BG-25	Quartz	11.0	610**	9.2 (q)
	Orthoclase	9.8		
<i>Pravo-Urmi deposit</i>				
U-143-88	Topaz from greizens	8.2	450- 550*	8.0-8.6 (t)
U-2-87	Topaz from cassiterite-topaz vein		380 - 480*	8.1-9.1 (t)
<i>Blizhnee deposit</i>				
BSHYU-1-14	Quartz	13.0	380***	8 (q)
	Cassiterite	3.0		

*Estimation on TBGCH of inclusions; ** calculation on (Chacko et al., 2001); ***Calculation on (Polyakov et al., 2005); (q) calculation on Clayton et al., 1972; (t) Calculation on (Zheng, 1993).

Oxygen isotope composition. The oxygen isotope composition was determined in coexisting quartz and orthoclase from granite of the Verkhneurmiisky pluton, in topaz from cassiterite–topaz veinlets of the Pravourmiisky deposit, and in coexisting quartz and cassiterite of the Blizhnee deposit (Table 4). The $\delta^{18}\text{O}$ values of quartz and orthoclase are similar, 1.2 and 1.3‰, respectively. The $\delta^{18}\text{O}$ values of topaz from the greisen and from the cassiterite–topaz vein differs by 0.9‰.

Conclusions and discussion. In contrast to the whole rock composition, the glass composition from melt inclusions makes it possible to estimate the content of water and other volatiles in magma from which granites of the Verkhneurmiisky pluton crystallized. Some differences in the composition of glasses from melt inclusions in quartz and granite hosting this quartz should be noted. The bulk rock compositions are slightly shifted with respect to the glass compositions of melt inclusions. The alkali content in glasses is also variable total alkali is between 6 and 9 wt %. Granites have lower Na_2O and stable K_2O , whereas the Na_2O and K_2O contents in glasses are higher and slightly lower, respectively, than those in granites.

Water. Two different trends with positive (A) and negative (B) correlations are clearly seen on the H_2O vs. SiO_2 diagram (Fig.1). Trend A corresponds to crystallization differentiation of a melt primarily undersaturated in water (~6 wt % H_2O) in a deep-seated magma chamber. When a condition close to water saturation was reached (~10–11 wt %), the granite melt ascended, accompanied by fluid loss (decompression boiling, trend B in Fig. 1a).

Chlorine and fluorine. Variable Cl and F concentrations in glasses and rocks (Tables 1, 2) indicate that these halogens were removed from the granite melt as it crystallized and degassed. Two inclusion groups are seen on the Cl vs. SiO_2 diagram (Fig. 8b). One of them (rhombs in Fig. 1b) shows increasing Cl as the SiO_2 concentration increases.

This tendency is consistent with trend A in Fig. 1a. The other group is close to the constant mean value, 0.08 wt %. This group with lower Cl concentration is consistent with trend B. The observed difference is apparently caused by two factors: (1) preferable Cl extraction with respect to H_2O by a fluid separated at the early evolutionary stage of the magmatic–fluid system and (2) immiscibility of the initially homogeneous fluid at a low pressure, which buffers the Cl content in the melt (i.e., the melt–aqueous solution–vapor system becomes invariant at a specific pressure (Shinohara, 1994).

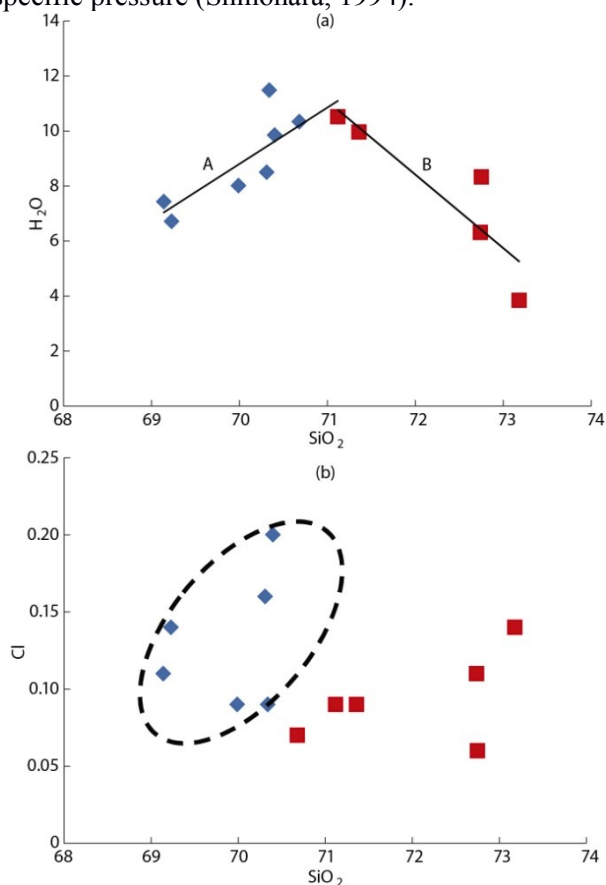


Fig. 1a, b. Binary diagrams: (a) H_2O vs. SiO_2 and (b) Cl vs. SiO_2 for melt inclusions. Rhombs depict composition of inclusions trapped in deep-seated chamber; squares

The formation and differentiation of magmas

depict composition of inclusions trapped during decompression and shallow crystallization.

The evolution of the fluid system. Variations in the SiO₂, H₂O, and Cl contents in glasses made it possible to reconstruct the PT and fluid evolution in the granite melt/magma. To this end, we calculated the crystallization differentiation of the model granite, whose simplified composition corresponds to the composition of sample BG-105 (Table 1) normalized to the ternary system Ab–Kfs–Qtz + 3.5 wt% H₂O. The calculations were made with DOMINO software (de Capitani and Petrakakis, 2010) and the thermodynamic database of Holland and Powel (2011) for minerals and granitic melt. The highest water content estimated in glasses (10–11 wt %) corresponds to a pressure of ~5 kbar (Holtz et al., 2001; Holland et al., 2018).

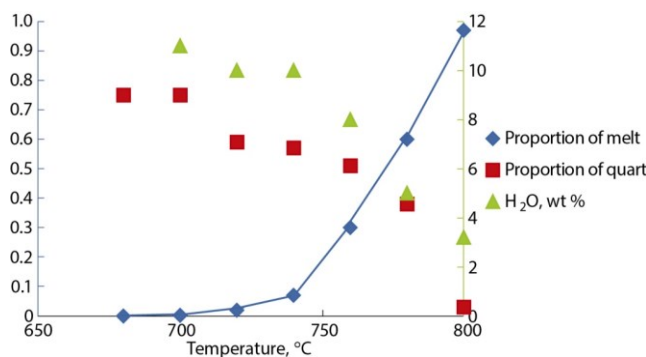


Fig. 2. Evolution of molar quantities (left scale) of melt (rhombs), quartz (squares), and water content in melt (wt %, triangles, right scale) with temperature.

Garnet reported by Gonevchuk (2000), which is formed as the peritectic phase of granitic melt under pressure as high as 5 kbar (Ellis, 1986), supports deep-seated melt chambers of the Verkhneurmiisky granitoid pluton. This value is adopted to estimate differentiation in a deep-seated chamber corresponding to trend A (Fig. 1a). The calculations show (Fig. 2) that quartz is the first crystallized phase on the liquidus temperature for the chosen bulk composition; it starts to crystallize slightly above 800°C. This is the highest temperature of melt inclusion entrapment. The H₂O content in the melt (~4 wt %, Fig. 2) calculated at 800°C, however, differs substantially from that in the glass of this sample (Table 2). The H₂O content of 8.2 wt % is more consistent with the value calculated at 760°C, when the melt proportion is about 0.3. A state of the melt close to water saturation (10 wt %) was attained at 740°C with a proportion of 0.1. The inclusions with the highest water content in the melt most likely were trapped at this temperature, then the decompression stage in the evolution of the magmatic–fluid system began. Adiabatic (i.e., close to isothermal) ascent of magma resulted in a drastic decrease in the H₂O content of the melt. The lowest

H₂O content in glass (3.84 wt %, Table 2) corresponds to a pressure of ~1 kbar (Holtz et al., 2001); in other words, magma lost more than 60% of dissolved fluid during its ascent. The temperature of 740°C is only 20° higher than that of the granite solidus temperature at one kbar (Holtz et al., 2001). It is within this narrow temperature range, granite finally crystallized and last fluid portions were separated.

The approximate pressure of the final melt crystallization and fluid separation has been estimated from the homogenization temperature of fluid inclusions of type 1 in igneous quartz and density of the trapped fluid. If we assume that these fluid inclusions were synchronously trapped with the melt inclusions at a temperature close to that of complete granite crystallization (680–720°C), then the isochore corresponding to these inclusions yields a pressure of 1.5 ± 0.1 kbar extrapolated to the high temperature (4.55 bar/°C; Knight and Bodnar, 1989). This value is consistent with the aforementioned pressure estimated from the lowest water content in glass.

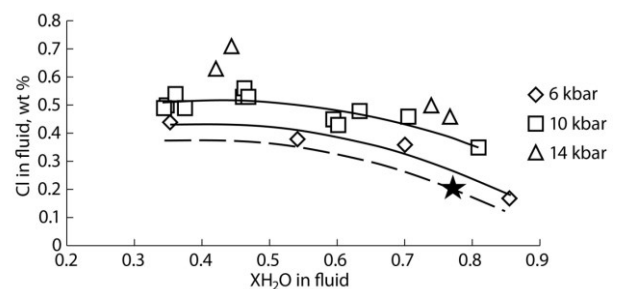


Fig. 3. Cl in melt versus XH₂O in fluid diagram showing composition of aqueous–salt fluid with K/(K + Na) ratio of 0.2–0.25. Experimental data (Aranovich, 2013) at various pressures are shown by symbols. Solid curves show interpolated experimental data. Dashed curve shows extrapolation to 5 kbar. Asterisk shows fluid composition in fluid inclusion from sample BG-105(5) in Table 2.

The salinity of fluid separated from granite in a deep-seated chamber was estimated from experimental data (Aranovich et al., 2013). The highest chlorine concentration in the fluid-saturated melt and Cl/H₂O ratio were 0.2 wt % and approximately 0.02, respectively (Table 2).

Fluid separated from magma contained CO₂ and methane. It is possible that these inclusions enriched in nonpolar gases were probably trapped due to immiscibility in the H₂O– nonpolar gas–strong electrolyte system (Aranovich et al., 2010; Aranovich, 2013).

Based on calculated data, the highest chlorine concentration in the fluid-saturated melt and Cl/H₂O ratio were 0.2 wt % and approximately 0.02, respectively (Table 2). Extrapolating the experimental data of Aranovich et al. (2013) down to 5 kbar (estimated from the highest H₂O content in the

granitic melt), the salinity of fluid initially separated from the melt was close to 50 wt % NaCl equiv. (Fig. 3)

Isotope system. The temperature (580 and 610°C, Table 4) estimated from the quartz–feldspar pair from samples of Badzhal granite reflects the closure temperature of quartz, in which the oxygen diffusion rate is lower than that in feldspar for the same *PT* parameters (Giletti, 1985).

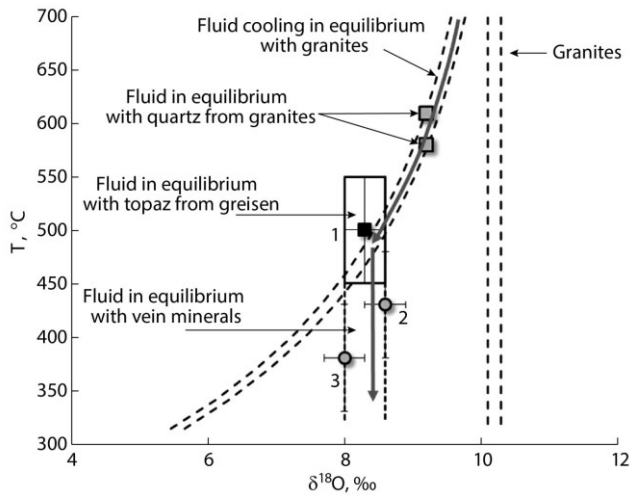


Fig. 4. Temperature vs. $\delta^{18}\text{O}$ diagram showing evolution of oxygen isotope composition during granite cooling and vein and greisens formation (Zharikov et al., 1992) calculated for Badzhal magmatic–fluid system ($\delta^{18}\text{O}(\gamma) = 10.2\text{‰}$). Right-angle fields were constructed for *T* and $\delta^{18}\text{O}(\text{fl})$ values given in Tables 3 and 4. (1) Fluid in equilibrium with topaz; (2, 3) fluid in equilibrium with vein minerals.

Figure 4 shows the calculated trend of the oxygen isotope composition of aqueous fluid equilibrated with the cooling Verkhneurmiisky granites and minerals from greisen and veins is shown. The proposed model of the magmatic–fluid system implies that no substantial amount of exotic fluid was involved in this system at all stages of its evolution, from fluid separation during granite crystallization to the formation of quartz veins (Zharikov et al., 1992). The $\delta^{18}\text{O}(\text{fl})$ value of fluid in equilibrium with topaz from greisens at the Pravourmiisky deposit was plotted on this diagram. Taking into account uncertainties of temperatures estimated from homogenization of fluid inclusions, it falls on the compositional curve of fluid in equilibrium with the Verkhneurmiisky granites. This is similar to the model of the Akchatau W–Mo deposit: the oxygen isotope composition of fluid in equilibrium with greisens minerals was consistent with that of fluid in equilibrium with granites. That model (Zharikov et al., 1992) suggested that greisen formation was the crucial stage in the evolution of the fluid system, before which the fluid had been governed by the exchange reaction with cooling granites (rock-dominated regime). After greisen crystallization, the

evolution of the fluid isotope composition was determined by its isotopic exchange with minerals from veins in the fluid-dominated regime. The diagram in Fig. 4 shows the evolution of fluid isotope exchange (arrows) and the estimated $\delta^{18}\text{O}(\text{fl})$ values of vein minerals (topaz, quartz) from the Pravourmiisky and Blizhnee deposits, which fall into the field of fluid in equilibrium with vein minerals predicted by the model.

Conclusions. The obtained results support a genetic relation between the Verkhneurmiisky and Blizhnee deposits and emplacement and crystallization of the Verkhneurmiisky granites, which are parts of Badzhal batholith (Gonevcuk et al., 2002).

The evolution of the composition of melts occurred as a result of crystallization differentiation at two structural levels: in a deep (about 15 km) magmatic chamber and in relatively shallow conditions (about 4 km). The change in the composition of the melts caused the evolution of the fluid separated from them from brine to the late supercritical, captured by igneous quartz and then topaz. The results show that the formation of greisens and veins of the Pravourmiiskoe and Blizhnee deposits is the result of the development of a single magmatic–fluid system, the origin of which was associated with the formation of the Pravourmiisky granite massif which is the dome of the Badzhal batholith. The behavior of volatiles - chlorine, fluorine and water at different stages of the evolution of the magmatogenic–fluid system is shown. The data obtained from the study of melt and fluid inclusions correspond to the calculated parameters made with DOMINO software. Behavior and role of volatiles in the crystallization of granites plays a significant role in the formation of a mineral-forming fluid and the transfer of metals.

The obtained estimates of the temperature of final crystallization of granites of the Verkhneurmiisky massif are quite comparable with the parameters of formation of tin-bearing granites of Erzebirge (~700 °C at depths of 3–6.5 km). They are also similar to the solidification conditions of intrusions in the tin-porphyry magmatogenic–fluid systems of Bolivia at temperatures between 620 and 740 °C.

Thus, a direct transition from the magmatic to the hydrothermal stage was established during the crystallization of rocks from the granitoid melt of the Badzhal tin-tungsten batholith and associated deposits.

References

- Aranovich, L. Ya., Fluid–mineral equilibria and thermodynamic mixing properties of fluid systems, *Petrology*, 2013, vol. 21, no. 6, pp. 539–549.
- Aranovich L. Ya., Zakirov, I. V., Sretenskaya, N. G., and Gerya, T. V., Ternary system H₂O–CO₂–NaCl at

The formation and differentiation of magmas

- high T–P parameters: an empirical mixing model, *Geochem. Int.*, 2010, vol. 48, no. 5, pp. 446–455. et al., 2010
- Chacko, Thomas. and David, R., Cole, and Juske Horita. Equilibrium oxygen, hydrogen and carbon isotope fractionation factors applicable to geologic systems, *Rev. Mineral. Geochem.*, 2001, vol. 43, no. 1, pp. 1–81.
- Clayton, R.N., O’Neil, J.R., and Mayeda, T.K., Oxygen isotope exchange between quartz and water, *J. Geophys. Res.*, 1972, vol. 77.
- Darbyshire, D.P.F. and Shepherd, T.J., Chronology of granite magmatism and associated mineralization, SW England, *J. Geol. Soc. London*, 1985, vol. 142, pp. 1159–1177.
- De Capitani, C. and Petrakakis, K., The computation of equilibrium assemblage diagrams with Theriak/Domino software, *Am. Mineral.*, 2010, vol. 95, pp. 1006–1016.
- Devine, J.D., Gardner, J.E., Brack, H.P., et al., Comparison of microanalytical methods for estimating H₂O contents of silicic volcanic glasses, *Am. Mineral.*, 1995, vol. 80, pp. 319–328.
- Dietrich, A., Lehmann, B., and Wallianos, A., Bulk rock and melt inclusion geochemistry of Bolivian tin porphyry systems, *Econ. Geol.*, 2000, vol. 95, no. 2, pp. 313–326.
- Ellis, D.J., Garnet-liquid Fe²⁺–Mg equilibria and implications for the beginning of melting in the crust and subduction zones, *Am. J. Sci.*, 1986, vol. 286, no. 10, pp. 765–791.
- Jiletti, B.J., The nature of oxygen transport within minerals in the presence of hydrothermal water and the role of diffusion, *Chem. Geol.*, 1985, vol. 53, pp. 197–206.
- Gonevchuk, V.G., Olovonosnye sistemy Dal’nego Vostoka: magmatizm i rudogenez (Tin Systems of the Far East: Magmatism and Ore Genesis), Vladivostok: Dal’nauka, 2002.
- Gonevchuk, V.G., et al., Hinggan–Okhotsk metallogenic belt in the terrane concepts, Rudnye mestorozhdeniya kontinental’nykh okrain (Ore Deposits of Continental Margins), Vladivostok: Dal’nauka, 2000, vol. 1, pp. 35–54.
- Holland, T.J.B. and Powell, R., An improved and extended internally consistent thermodynamic dataset for phases of petrological interest, involving a new equation of state for solids, *J. Metamorph. Geol.*, 2011, vol. 29, pp. 333–383.
- Holland, T.J.B., Green, T.C.R., and Powell, R. Melting of peridotites through to granites: a simple thermodynamic model in the system KNCFMASH+TOCr, *J. Petrol.*, 2018, vol. 59, no. 5, pp. 881–900.
- Holtz, F., Johannes, W., Tamic, N., et al., Maximum and minimum water contents of granitic melts generated in the crust: a evaluation and implications, *Lithos*, 2001, vol. 56, pp. 1–14.
- Knight, C.L. and Bodnar, R.J., Synthetic fluid inclusions: IX. Critical PVTX properties of NaCl–H₂O solutions, *Geochim. Cosmochim. Acta*, 1989, vol. 53, pp. 3–8.
- Kovalenko, V.I., Petrologiya i geokhimiya redkometal’nykh granitoidov (Petrology and Geochemistry of Rare-Metal Granites), Novosibirsk: Nauka, 1977.
- Le Maitre, R.W., et al., *Igneous Rocks: a Classification and Glossary of Terms: Recommendations of the International Union of Geological Sciences Subcommission on the Systematics of Igneous Rocks*, Cambridge University Press, 2005.
- Maniar, P.D. and Piccoli, P.M., Tectonic discrimination of granitoids, *Geol. Soc. Am. Bull.*, 1989, vol. 101, pp. 635–643.
- Nielsen, C.H. and Sigurdsson, H., Quantitative methods for electron micro-probe analysis of sodium in natural and synthetic glasses, *Am. Mineral.*, 1981, vol. 66, pp. 547–552.
- Polyakov, V.B., Mineev, S.D., Clayton, R.N., Hu, G., Gurevich, V.M., Khramov, D.A., Gavrichev, K.S., Gorbunov, V.E., and Golushina, L.N., Oxygen isotope fractionation factors involving cassiterite (SnO₂): I. Calculation of reduced partition function ratios from heat capacity and X-ray resonant studies, *Geochim. Cosmochim. Acta*, 2005, vol. 69, pp. 1287–1300.
- Roedder, E., *Fluid Inclusions*. Rev. Mineral., Washington: Mineral. Soc. Am., 1984, vol. 12.
- Shinohara, H., Exsolution of immiscible vapor and liquid phases from a crystallizing silicate melt: implications for chlorine and metal transport, *Geochim. Cosmochim. Acta*, 1994, vol. 58, no. 23, pp. 5215–5221.
- Smirnov, S. Z., Bortnikov, N. S., Gonevchuk, V. G., and Gorelikova, N. V., Melt compositions and fluid regime of crystallization of rare-metal granite and pegmatites from the Sn–W Tigrinoe Deposit (Primor’e), *Dokl. Earth Sci.*, 2014, vol. 456, no. 1, pp. 558–562.
- Thomas, R. and Klemm, W., Microthermometric study of silicate melt inclusions in Variscan granites from SE Germany: volatile contents and entrapment conditions, *J. Petrol.*, 1997, vol. 38, no. 12.
- Zharikov, V.A., Dubinina, E.O., Shapovalov, Yu.B., and Suvorova, V.A., Origin of ore-bearing fluid of the Akchatau rare-metal deposit, *Geokhimiya*, 1992, no. 2, pp. 163–170.
- Zheng, Y.F., Calculation of oxygen isotope fractionation in hydroxyl-bearing silicates, *Earth. Plan. Sci. Lett.*, 1993, vol. 120, pp. 247–263.

Persikov E.S., Bukhtiyarov P.G., Shchekleina M.D. Features of basalt melt crystallization at moderate hydrogen pressures (preliminary results).

IEM RAS. Chernogolovka. persikov@iem.ac.ru

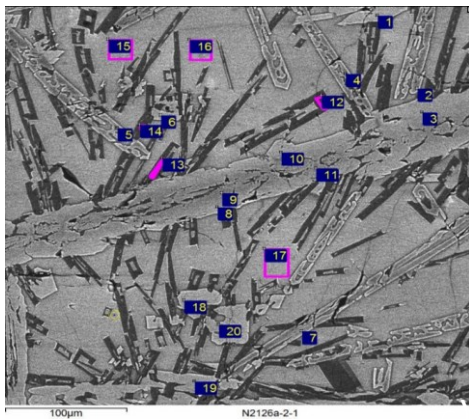
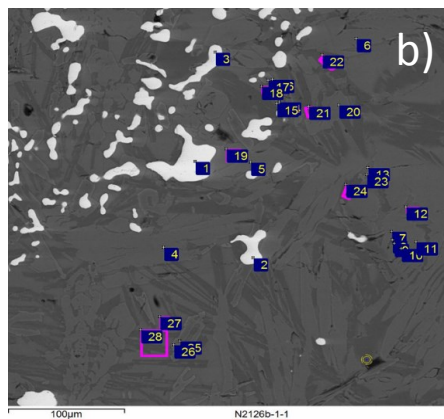
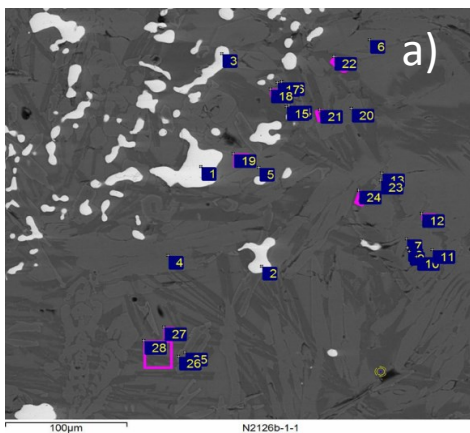
Abstract Important problems of magma differentiation, the formation of native metals and ore formation processes in the earth’s crust, are increasingly associated with the active participation of hydrogen. In this paper, new experimental data obtained on the crystallization of basalt melts at high temperatures (1100–1250 °C) and hydrogen pressures (10–100 MPa) are presented, which clarify the possible role of hydrogen in the processes occurring in basalt melts in the earth’s crust and during volcanism under highly reduced conditions ($f(\text{O}_2) = 10^{-14}$). In

crystallization experiments, it was found that the compositions of crystals (olivines, clinopyroxenes and plagioclases) formed in the experiment on the crystallization of a melt of magnesium basalt under hydrogen pressure closely correspond to the compositions of crystals of lava flows of the Northern breakout of Tolbachik volcano in Kamchatka. This result can be considered as an experimental confirmation of the participation of hydrogen in the volcanic process.

Keywords: basaltic melt, hydrogen, pressures, temperature, native metal, crystallization, reducing conditions

The role of hydrogen, the most common element of our Galaxy, in natural processes is extremely diverse and in recent years has attracted increasing attention of petrologists and geochemists. Important problems of magma differentiation, the formation of native metals, and ore formation processes in the earth's crust are increasingly associated with the active participation of hydrogen (Bird et al., 1981; Ryabov et al., 1985; Oleynikov et al., 1985; Marakushev, 1995; Levashov and Okrugin, 1984; and others). Recently, we have obtained the first results on experimental modeling of the formation of native metals in the earth's crust when hydrogen interacts with basaltic melts and on the kinetics of basaltic magma differentiation under hydrogen pressure (Persikov et al., 2019). In this paper, new experimental data obtained on the crystallization of basalt melts at high temperatures (1100-1250 °C) and

hydrogen pressures (10-100 MPa) are presented, which clarify the possible role of hydrogen in processes occurring in basalt melts in the earth's crust and during volcanism under highly reductive conditions. The experiments were carried out using a unique high gas pressure equipment. This unit is equipped with an original internal device (Persikov et al., 2019), which made it possible to conduct long-term experiments at such high temperatures, despite the high penetrating power of hydrogen. Two types of experiments were performed at different hydrogen pressures: 1-simulation of the movement of basaltic magma from hypabyssal facie to near-surface conditions in an isothermal mode corresponding to a volcanic eruption (Fig. 1a); 2-crystallization of displaced basaltic magma in near-surface conditions corresponding to a volcanic eruption (Fig. 1b, c.). In both types of experiments, it was found that, despite the high reduction potential of the H₂ – basalt melt system, the reactions of hydrogen oxidation and complete reduction of Fe oxides in the melt do not end. As a result, the initially homogeneous basalt melt becomes heterogeneous (Table 1): H₂O is formed in the fluid phase (initially pure hydrogen); H₂O is dissolved in basalt melts, and small metal separations of the liquation structure are formed at a temperature significantly lower (1250 °C) than the melting point of the metal phases (Fe, 1560 °C).



a) run No. 2128, experiment with melts of starting magnesium basalt, $P(\text{H}_2) = 100 \text{ MPa}$, $T = 1250 \text{ }^\circ\text{C}$, run duration is 1 hr, then decreasing of hydrogen pressure to 10 MPa at the isothermal condition, run duration is 1 hr, and then isobaric quenching (white color is metallic alloy of Fe, black color is basaltic glass, composition - see table 1).

b) run No. 2126, experiments with melts of starting magnesium basalt, $P(\text{H}_2) = 100 \text{ MPa}$, $T = 1250 \text{ }^\circ\text{C}$, run duration is 1 hr, then decreasing of hydrogen pressure to 10 MPa at the isothermal condition, run duration is 1 hr, then temperature decreasing to 1100 °C at the isobaric condition, run duration is 2 hr (crystallisation) and then isobaric quenching (white color is metallic alloy of Fe, the composition – see table 2, light grey color is residual glass, composition - see table 1, black gray color are crystals: olivine, clinopyroxene, plagioclase).

c) run No. 2126, the result of crystallization of magnesium basaltic melt (2,5,7- olivines; 3, 10,11,18,19,20 – clinopyroxenes; 12,13,14 – plagioclases; 15,16,17 – glass).

Fig. 1. Backscattered electron image of the quenching samples after experiments on the interaction of basaltic melts with hydrogen.

The formation and differentiation of magmas

Table 1. Chemical composition (wt. %) and the structural-chemical parameter (100NBO/T) of the starting basalt and basaltic glass (average composition) after experiments under hydrogen pressure.

Components	2128*	2126**	The composition of the starting basalt***
SiO ₂	54.05	55.86	49.5
Al ₂ O ₃	14.79	16.75	13.18
Fe ₂ O ₃	0.00	0.00	3.18
FeO	4.32	6.79	6.85
MnO	0.16	0.15	0.15
MgO	9.26	3.41	9.98
CaO	12.36	9.68	12.34
Na ₂ O	2.65	3.34	2.18
K ₂ O	1.0	1.96	0.93
TiO ₂	1.17	1.26	1.01
P ₂ O ₅	no	0.2	0.25
no	no	no	no
H ₂ O-	0.34	0.34	0.29
NiO	0.07	0.07	no
Co ₃ O ₄	0.1	0.1	no
Sum	100.27	99.91	99.84
100NBO/T	74	44	83

Note: Water content determined by Karl-Fisher titration method.

*- Experiments with melts of starting magnesium basalt, $P(\text{H}_2) = 100 \text{ MPa}$, $T = 1250 \text{ }^\circ\text{C}$, run duration is 1 hr, then decreasing of hydrogen pressure to 10 MPa at the isothermal condition, run duration is 1 hr, and then isobaric quenching.

** - Experiments with melts of starting magnesium basalt, $P(\text{H}_2) = 100 \text{ MPa}$, $T = 1250 \text{ }^\circ\text{C}$, run duration is 1 hr, then decreasing of hydrogen pressure to 10 MPa at the isothermal condition, run duration is 1 hr, then temperature decreasing to 1100 °C, run duration is 2 hr (crystallization) and then isobaric quenching.

*** - Big Tolbachinsky fissure eruption 1975-1976, Kamchatka, 1984 (Fedotov et al., 1984).

Equation (1) and measured amounts of H₂O dissolved in the melt (0.34 wt.) were used to estimate the oxygen fugacity corresponding to the termination of redox reactions in melts in the crystallization experiment (No. 2126), Table 1).

$$f(\text{O}_2) = [f(\text{H}_2\text{O}) / ((f(\text{H}_2) * \exp(-\Delta G_o(1)/RT))]^2, \quad (1)$$

Under experimental conditions (1100 °C/10 MPa), the binary fluid (H₂O-H₂) is close to ideal, so that $f(i) = X(i) * P$. Given that $X(\text{H}_2\text{O}) + X(\text{H}_2) = 1$ and $\Delta G_o(1, 1373\text{K}) = -343.6 \text{ kJ}$ (Barin, 1995), the solution of equation (1) leads to the value of $\log f(\text{O}_2) = -14.1$, i.e. we have highly reductive conditions in the experiment, about an order of magnitude less than the iron/wustite buffer.

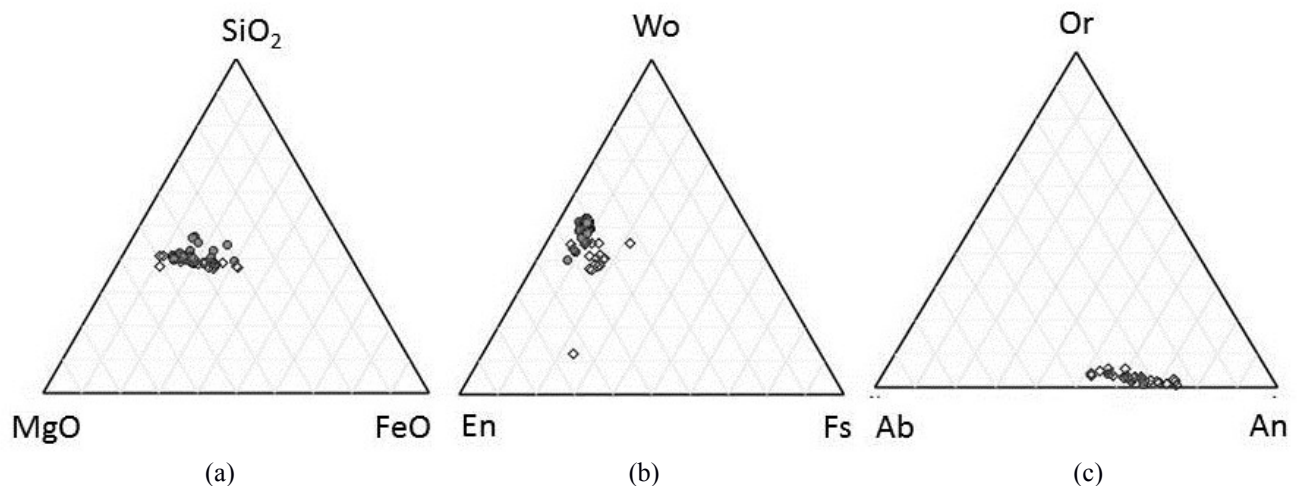


Fig. 2. Comparison of the composition of crystals formed in experiment No 2126 (closed symbols), with that of natural minerals (open symbols) from magnesium basalt lava flows of the Large Tolbachik eruption 1975-1976, Kamchatka (Fedotov et al., 1984).

(a) - olivines, experimental: $\text{Fo}(\text{max}) = 86$, $\text{Fo}(\text{min}) = 65$; natural: $\text{Fo}(\text{max}) = 89$, $\text{Fo}(\text{min}) = 63$.

(b) clinopyroxenes (average) - experimental: $\text{Wo} = 49.64$, $\text{En} = 42.31$, $\text{Fs} = 8.06$; natural: $\text{Wo} = 40.55$, $\text{En} = 45.16$, $\text{Fs} = 14.29$.

(c) - plagioclases (average) - experimental: $\text{An} = 62.24$, $\text{Ab} = 35.44$, $\text{Or} = 2.32$; natural: $\text{An} = 63.27$, $\text{Ab} = 33.77$, $\text{Or} = 2.97$.

In crystallization experiments, it was found that the compositions of crystals (olivines, clinopyroxenes and plagioclases) formed in the

experiment on the crystallization of the melt of magnesium basalt closely correspond to the compositions of crystals of lava flows of the

Northern breakout of Tolbachik volcano in Kamchatka (Fig.2). This result can be considered as an experimental confirmation of the participation of hydrogen in the volcanic process, which is also consistent with the composition of volcanic gases detected (Fedotov et al., 1984).

References

- Barin, I. 1995. Thermochemical Data of Pure Substances. Third Edition. VCH Publishers, Inc., New York, USA, pp. 1885.
- Bird J.M., Goodrick C.A., Weathers M.S. (1981) Petrogenesis of Uivuaq iron, Disko Island, Greenland. *J. Geophys. Res.* B 86 (12), 11787-11806.
- Fedotov S.A. et al., (1984) Tolbachinskii a large fissure eruption 1975-1976, Kamchatka (1984), Moscow: Nauka, 637 p. (in Russian).
- Levashov V. K., Okrugin, B. V. (1984) Evaluation of the physical conditions for the formation of segregations of native iron in basaltic melt. *Geochemistry and Mineralogy of mafics and ultramafics of the Siberian platform.* Yakutsk, 54-62 (in Russian).
- Marakushev A. A. (1995) Nature of native metals formation. *Dokl. RAS*, vol. 341, No. 6, 807-812.
- Native metals in igneous rocks (1985) All-Union conference. Abstracts, part 1. Ed. B. V. Oleynikov. Yakutsk: YB of USSR Acad. Sci. 188 p. (in Russian).
- E.S. Persikov, P.G. Bukhtiyarov, L.Ya. Aranovich A.N., Nekrasov, O.Yu. Shaposhnikova (2019) Experimental modeling of formation of native metals (Fe,Ni,Co) in the earth's crust by the interaction of hydrogen with basaltic melts. *Geochemistry International*, Vol. 57, No. 10, pp. 1035–1044.
- Ryabov V. V., Pavlov A. L., Lopatin G. G. (1985) Native iron in Siberian traps. Novosibirsk: Nauka SB RAS, 167 p. (in Russian).

Rusak A.A.¹, Shchekina T.I.², Alferyeva Ya.O.², Gramenitskiy Eu.N.², Zinovieva N.G.², Khvostikov V.A.³, Kotelnikov A.R.⁴ Features of phase crystallization in a high-fluorine model granite system at a temperature drop from 700 TO 400 °C and a pressure of 1 kbar UDC 552.11, 550.42.

¹Vernadsky Institute of Geochemistry and analytical chemistry RAS (GEOKHI RAS), Moscow,

²Lomonosov Moscow State University, Department of Geology, Moscow,

³Institute of problems of technology of microelectronics and special-purity materials RAS (IPTM RAS),

⁴Korzhiński Institute of Experimental Mineralogy RAS (IEM RAS), Chernogolovka (aleks7975@yandex.ru, t-shchekina@mail.ru; yanaalf@yandex.ru, engramen@geol.msu.ru, khvos@ipmt-hpm.ac.ru, nzinov@mail.ru, kotelnik@iem.ac.ru).

Abstract. A series of experiments was performed in a high-fluorine model granite system Si-Al-Na-K-Li-F-O-H at temperatures of 700, 600, 550, 500 and 400 °C and a pressure of 1 kbar. The experiments were carried out on a high gas pressure unit at the Institute of Experimental

Mineralogy of Russian Academy of Sciences. It is shown that when the temperature decreases, the phase relations in the system change. At T=800 °C and P=1 and 2 kbar, the equilibrium phases are aluminosilicate (L) and aluminofluoride salt (LF) melts and an aqueous fluid (FI) with a water content of ~10 wt.%. When the temperature drops to 700 °C, the salt melt partially crystallizes to form large crystals of aluminofluorides (cryolite - CrI and cryolitionite), which practically do not contain REE. At a temperature of 600 °C and a pressure of 1 kbar, quartz (Qtz) crystallizes from the aluminosilicate melt and the equilibrium becomes as follows: L+LF+CrI+Qtz. The residual salt melt that concentrated most REE is preserved up to T=500 °C and P=1 kbar. At a temperature of 500 °C and a pressure of 1 kbar, quartz and fluorine-containing aluminosilicate crystallize from the aluminosilicate melt, which is comparable in appearance and chemical composition to polyolithionite. Experiments were also performed at 400 °C and 1 kbar. According to preliminary data, the products of experiments still contain aluminosilicate glass, which, apparently, is in metastable state.

Keywords: granite system, rare earth elements, fluorine, temperature, pressure, aluminosilicate, aluminofluoride, salt melts, water content, pressure effect, temperature effect.

The aim of this work was to study the sequence of phase crystallization in the high-fluorine model granite system Si-Al-Na-K-Li-F-O-H at a temperature drop from 700 to 400 °C and a pressure of 1 kbar and at different water content.

The compositions of the solid charge for experiments were set based on the composition of the aluminosilicate melt with certain ratios of Si, Al, Na+K+Li and the fluoride salt phase (cryolite) in an amount sufficient to saturate the aluminosilicate melt. The initial composition of the silicate melt corresponded to the granite eutectic of the quartz-albite-orthoclase system containing 1 wt. % F (Manning, 1981) and 1.5 wt. % Li at a temperature of 690 °C and a pressure of 1 kbar H₂O.

The following reagents were used to prepare the initial compositions for experiments at T = 700, 550, 500 and 400 °C and P =1 kbar: dried gel SiO₂, LiF, K₂SiF₆, NaF, AlF₃, Al₂SiO₅, Al₂O₃ and distilled water. Rare earth elements (REE) La, Ce, Pr, Nd, Sm, Eu, Gd, Tb, Dy, Ho, Er, Tm, Yb and Lu, as well as yttrium (Y) and scandium (Sc) were introduced as oxides of 0.5 wt. % elements. From 10 to 50 wt. % distilled water was added depending on the weight of the attachment. For experiments set at a temperature of 600 °C and a pressure of 1 kbar, rare earth oxides were introduced into the system in certain pairs so that the instrument did not overlap the REE peaks (1) Y₂O₃, La₂O₃; (2) Sm₂O₃, Gd₂O₃, Tb₂O₃; (3) CeO₂, Eu₂O₃ and Ho₂O₃; (4) Dy₂O₃; (5) Pr₂O₃, Lu₂O₃, Sc₂O₃; (6) Er₂O₃, Yb₂O₃; (7) Nd₂O₃, Tm₂O₃; (8) Sc₂O₃, Gd₂O₃ in quantities of 2 wt. % of the element by weight of the solid charge. Distilled water was added to each ampoule by 15 wt. % of the weight of the hitch. The ratios of reagents were selected so that

The formation and differentiation of magmas

the expected aluminosilicate melt in the experimental products was close to the compositions of highly evolved Li-F and cryolite-bearing granites. The starting materials were thoroughly mixed in agate mortar in an atmosphere of alcohol and placed in a platinum ampoule, which was administered distilled water. The size of ampoules in length was up to 25 mm, external diameter - 3 mm, wall thickness - 0.2 mm.

The experiments were carried out on a high gas pressure installation ("gas bomb") at the Institute of Experimental Mineralogy of the Russian Academy of Sciences in Chernogolovka (IEM RAS). The accuracy of temperature control and adjustment was ± 5 °C; pressure ± 50 bar. For each ampoule, mass control was performed before and after the experiment. The experiment was considered successful if the mass discrepancy was no more than 0.001 g. The experimental products were studied on a scanning electron microscope Jeol JSM-6480LV (Japan) with energy-dispersion INCA Energy-350 and crystal-diffraction INCA Wave-500 (Oxford Instrument Ltd., UK) spectrometer in the laboratory of local methods of substance research of the Department of Petrology and Volcanology of Moscow State University. The accelerating voltage was 20 keV at a current of 0.7 nA. The main and rare earth elements in silicate glasses were studied using the Superprobe JXA-8230 electron probe microanalyzer (Japan). To prevent glass destruction, the analyses were performed in a defocused beam mode (up to 10 microns) at an accelerating voltage of 10 kV and a current of 10 nA. REE analysis was performed at an accelerating voltage of 20 kV and a current of 30 nA. Concentrations of rare earth elements, yttrium, scandium and lithium were determined by inductively coupled plasma mass spectrometry using the ICP MS double-focus Element-2 device in the laboratory of Experimental Geochemistry of the Department of Geochemistry of the faculty of Geology of Moscow State University (MSU). Due to the small amount of the analyzed substance, the concentrations were recalculated for the content of aluminum in the phases determined in advance by microprobe analysis.

As a result of the experiments performed when the temperature decreases from 700 to 400 °C with a pressure of 1 kbar, the phase relations in the model Si-Al-Na-K-Li-F-O-H granite system change, but at all parameters an aluminosilicate melt is formed, up to 400 °C.

When studying experimental products on the electron microscope at 700 °C it was determined that the main phase was an aluminosilicate melt (L), immersed in it salt globules (LF) of alkaline-aluminofluoriding composition, stoichiometry

cryolithionite crystals up to 100 μm in diameter (Fig. 1) and aqueous fluid (Rusak et al., 2019). The salt melt crystallizes during quenching and forms a polyphase aggregate of Li-Na-K - aluminofluoride crystals. Salt globules, in addition to alkaline aluminofluorides, are rich in REE, yttrium and scandium fluorides.

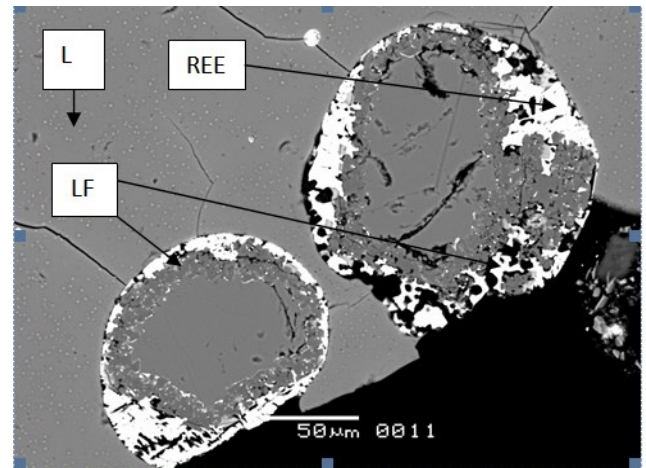


Fig.1. Salt globules (LF) with a diameter of 150 μm , the formed crystals aluminofluoride phase (like Li-containing cryolite), surrounded by seasoned salt melt of the rare-earth fluorides, located in the outer part of the globules at the border of aluminosilicate melt (L). REE – rare earth elements, Sc and Y.

The obtained results of experiments conducted at 700 °C show that when the temperature decreases from 800 to 700 °C, the system approaches the subsolidus, because in addition to the aluminosilicate and salt melts and water fluid, crystals of Li-bearing cryolite are also observed.

When the temperature dropped to 600 °C, the equilibrium phases were aluminosilicate melt, quartz, aluminofluoride salt melt, and Li-K-Na-cryolite phase that crystallized from the salt melt. The size of cryolite crystals reached 100-180 microns (Fig. 2). From the salt melt there also crystallizes the connection type, LiF - griset, ScF_3 , YF_3 and fluorides of other rare earths. The actual composition of the fluoride melt (excluding the water component) under experimental conditions is the total composition of the entire mixture of quenching phases. The main products of crystallization in experiments at 600 °C and 1 kbar in different experiments were quartz, cryolite and alkaline fluorine-bearing silicate mineral similar in composition to polyolithionite (Fig. 3), which forms a border around the globules of the salt phase with a width of about 150 – 200 microns. Their crystallization, especially of quartz, indicates that they are approaching the subsolidus of the system.

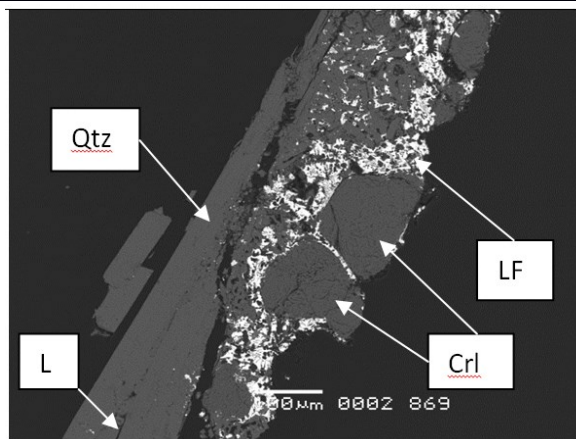


Fig. 2. Cryolite (CrI) (100-150 microns), crystallized from a salt melt (LF); quartz (Qtz) (up to 600 microns), crystallized from an aluminosilicate melt (L).

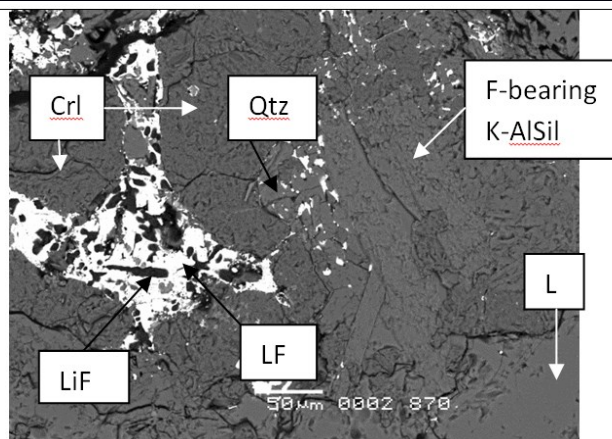


Fig. 3. Phases crystallized at 600 °C and 1 kbar in particular cryolite (CrI) (up to 100-125 microns), griset (LiF) (up to 50 microns in length) from salt melt (LF) and quartz (Qtz) (up to 25 microns), alkaline fluorine-bearing silicate (F-bearing K-AlSiI), presumably polyolithionite (up to 200 microns in length and 150 microns in width) from an aluminosilicate melt (L).

When the temperature decreases to 500 °C and at a pressure of 1 kbar and with water content of 10 wt. % the process of crystallization continues. At this temperature, the aluminosilicate and aluminofluoride melts and water fluid are in equilibrium. Quartz is crystallized from the silicate melt reaching 100 microns across. Crystals of Na-K cryolite are often formed inside them, which indicates the joint crystallization of quartz and Na-K aluminofluorides. Large crystals of aluminofluorides (cryolite) up to 90 microns crystallize inside the globules. Non-crystallized salt melt, which concentrates rare earth elements, is preserved in large globules up to 500 °C (Fig. 4). Thus, this can prove the possible existence of a salt phase melt at fairly low temperatures during the formation of large cryolite-bearing granite massifs containing REE.

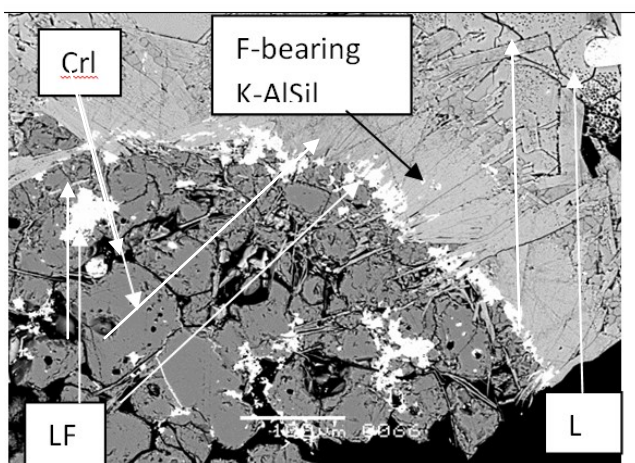


Fig. 4. Large crystals of cryolite (CrI) up to 90 microns in an uncrystallized salt melt (LF), which concentrated REE, and aluminosilicate glass (L), which are separated by potassium fluorine-bearing aluminosilicate (F-bearing K-AlSiI), the size of elongated crystals reaches 100 microns in length (T=500 °C).

In all experiments of this series, starting from the temperature of 600 °C, a border is formed between the salt and aluminosilicate melt, which corresponds to the composition of an alkaline fluorine-bearing silicate. At T = 500 °C, large elongated crystals up to 100 microns in length were formed (Fig. 4). According to preliminary data, the composition corresponds to mica, polyolithionite $KLi_2AlSi_4O_{10}F_2$, which is formed at low temperatures in pegmatites (for example, the Lovozero massif).

Rare earth elements form LnF_3 fluorides or complex fluorides with alkaline elements during salt melt quenching and are often formed in salt melt globules at the contact with the silicate melt.

Experiments were also performed at 400 °C and 1 kbar. When studying samples under binoculars, we discovered that the products of experiments still retain aluminosilicate glass, which, apparently, is in a metastable state.

Ultimately, it should be said that when the temperature decreases from 700 to 400 °C, the high-fluorine model granite system Si-Al-Na-K-Li-F-O-H approaches solidus with the formation of a typical paragenesis of minerals of cryolite-bearing granites. When conducting experiments, we approached the equilibrium "from above" from 800 °C to a given temperature, which is only possible if we used chemical reagents and not pre-prepared glasses as starting substances. It is likely that only partial crystallization of the silicate melt up to 400 °C and its metastable state is the result of supercooling of the viscous melt in experiments. At the same time, we were able to trace the features of crystallization of fluorine-rich granite melts, which are close analogues of cryolite-bearing granites, such as those forming the rare metal deposits of Ivigtut, Ulug-Tanzek, Katugin, etc., in which cryolite forms massive clusters and which are characterized by the presence

The formation and differentiation of magmas

of Li micas, similar to the mica that we obtained in experiments at 600 and 500 °C.

The work was supported by the Russian Foundation for Basic Research, grant № 16-05-00859.

References

- Manning D. The effect of Fluorine on liquidus phase bonds in the system Qz-Ab-Or with excess water at 1 kb // *Contrib. Mineral. Petr.* V. 76. 1981. pp. 206-215.
- Rusak A. A., Shchekina T. I., Gramenitsky E. N., Alferyeva Ya. O., Kotelnikov A. R., Bychkov A. Yu. Influence of pressure, temperature and water fluid on phase relations in the granite system. Collection of materials "New in the knowledge of ore formation processes: the Ninth Russian youth scientific and practical School with international participation", 2019, pp. 324-326.

Tobelko D.P.¹, Portnyagin M.V.^{1,2}, Krashennnikov S.P.¹ Complex methodology for estimating the primary H₂O content in island-arc magmas (the case of Kamchatka)

¹ Vernadsky Institute of Geochemistry and Analytical Chemistry RAS, Moscow, dariatobelko@gmail.com
² GEOMAR Helmholtz Centre for Ocean Research, Kiel, Germany

Abstract. The paper presents a new complex methodology for estimating crystallization temperatures and primary H₂O content in mantle island-arc magmas based on the analysis of coexisting olivine, chromium spinel and melt inclusions on the example of Eastern volcanic belt volcanoes, Kamchatka. The most primitive association of olivine and chromium spinel in basalts of Eastern Volcanic Belt of Kamchatka is crystallized at temperatures of 1030-1180°C, the pressure of 3-8 kbar, and oxygen volatility QFM+1.6. The average H₂O content in the most primitive melts is 4-8 wt %. Data on the Kumroch Volcanic Complex (Eastern Cones) were also taken into account when developing the methodology.

Keywords: *thermometry, H₂O, melt inclusion, olivine, parental magma, Kamchatka*

Introduction. The ocean lithosphere is recycled into the mantle in subduction zones and new lithosphere of continental type is formed, which determines the major role of subduction processes in geodynamics. The existing methods for estimation conditions of magma formation are based on the interpretation of the main, trace elements and volatile components contents in the parental mantle melt. One of the most important parameters for the composition of island-arc magmas is H₂O content in them (Portnyagin et al., 2007, Sobolev et al., 1996, etc.). The water content in melts is a very important parameter (Sisson, Grove, 1993; Lange et al., 1994; Sparks et al., 1994), which influences the temperature and crystallization order of minerals, shifts their compositions and directly influences the

evolution of the magmatic system. Therefore, the existing models of island-arc magmatism fundamentally depend on the accuracy of primary water content estimates in magma. The key to studying the composition of initial suprasubduction magmas is melt inclusions in minerals (Roedder, 1984). However, many years of investigations in studying melt inclusions revealed a number of problems (e.g., Danyushevsky et al., 2000; Gaetani and Watson, 2000, Portnyagin et al., 2008, Gaetani et al., 2012, Portnyagin et al., 2019). Initial H₂O content of island-arc magmas should be reviewed based on detailed studies of specific objects and application of independent methods for estimating initial H₂O content, since the measured water content in melt inclusions (the traditional method) does not correspond to the initial water content in magma (Nazarova et al., 2017, Portnyagin et al., 2019).

For magmas of Eastern Volcanic belt of Kamchatka, data on direct measurement of H₂O contents in primitive melt inclusions are extremely scarce (Portnyagin et al., 2007, Nazarova et al., 2017, Tobelko et al., 2019). The results obtained for Kamchatka volcanoes in recent years showed that previously estimated H₂O contents in melts are minimal (Mironov et al., 2015, Kamenetsky et al., 2017, Portnyagin et al., 2019, Tobelko et al., 2019). Therefore, it became necessary to use independent methods to revise the initial water content in the island-arc magmas in general and in the Eastern Volcanic belt of Kamchatka in particular.

In this work, a complex methodology for estimating the crystallization temperature and primary H₂O content in mantle island-arc magmas has been developed based on analysis of coexisting olivine, chromium spinel, and melt inclusions for 4 volcanoes of Eastern Volcanic belt of Kamchatka. Data on the Kumroch Volcanic Complex (East Cone) were also taken into account when developing the methodology.

Methodology. Melt inclusions in olivine were partially crystallized. Partial homogenization of the melt inclusions in olivine was performed for five minutes at atmospheric pressure, T = 1300°C, and oxygen fugacity corresponding to the buffer equilibrium Ni–NiO in a vertical tube furnace with a controlled oxygen fugacity Nabertherm RHTV 120-300/17 at the Vernadsky Institute, Russian Academy of Sciences (Krashennnikov et al., 2016). Measurements of the concentration of major elements in glasses melt inclusions, olivine and spinel were carried out on electron microprobe JEOL JXA 8200 (GEOMAR, Kiel, Germany). Determination of trace elements in olivine and melt inclusions was performed by inductively coupled plasma with laser ablation at Christian-Albrechts

University (Kiel, Germany). Details are described in Tobelko et al., 2019.

The method developed in this work for estimating primary H₂O content in mantle island-arc magmas is based on comparison of 3 calculation methods:

1-2) Estimation of initial H₂O content in melts was obtained using the method (Sobolev et al., 2016; Nazarova et al., 2017). The method is based on the significant influence of H₂O presented in the melt on olivine liquidus temperature. It allows to estimate initial H₂O content by comparing independently determined "real" (olivine-spinel (1) - Coogan et al., 2014; Sc/Y olivine-melt (2) -Mallmann, O'Neill, 2013) and "dry" (pseudo-liquidus - Ford et al., 1983) temperatures of olivine crystallization. The formula for estimating H₂O content was obtained by transformation of the dependence of olivine liquidus temperature on the water content in the melt (Almeev et al., 2007): $H_2O = (\Delta T/39.69)^{1.37}$, where ΔT is the difference between the dry liquidus temperature and the liquidus temperature in the presence of water (Fig.1).

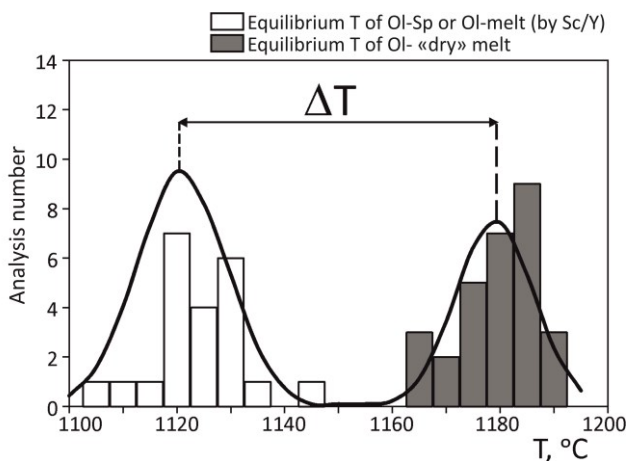


Fig.1. Evaluation of the initial H₂O content in melt inclusions. The figure shows an illustration of estimation method based on comparison of real temperatures estimated using olivine-spinel or Sc/Y thermometers and "dry" pseudo-liquidus temperatures of equilibrium between melt inclusions and olivine for Gorely volcano (Nazarov et al., 2017). Solid line - normal theoretical temperature distribution.

Results and discussion. The magma crystallization temperatures were estimated using an olivine-spinel Al geothermometer (Coogan et al., 2014) and a liquidus Sc/Y olivine-melt thermometer (Mallmann, O'Neill, 2013). Oxygen fugacity - using olivine-spinel oxybarometer (Ballhaus et al., 1991). Minimal pressure was estimated by the model (Shishkina et al., 2010). The initial water content was calculated using the new complex methodology described above.

As a result of investigations, it was found that the most primitive association of olivine and chromium

spinel in basalts of Eastern Volcanic belt of Kamchatka crystallized at temperatures of 1030-1180°C, the pressure of 3-8 kbar, and oxygen fugacity QFM+1.6. The average H₂O content in the most primitive melts is from 4 to 8 wt% (Fig. 2).

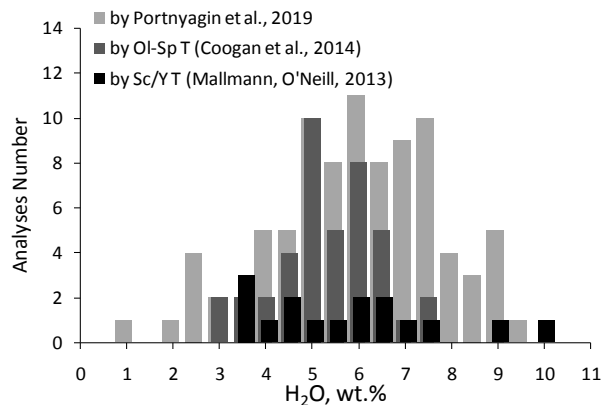


Fig. 2. Complex estimation of initial H₂O content in magmas of Eastern Volcanic belt of Kamchatka (Fo>85) based on a comparison of various calculation methods for water determination.

The estimates of initial H₂O content in magmas obtained in this work using a new methodology are 2–6 wt.% higher than previously expected (e.g., Sobolev, Chaussidon, 1994; Portnyagin et al., 2007). Our data also confirm the results obtained for Kamchatka volcanoes in recent years (Mironov et al., 2015, Kamenetsky et al., 2017, Portnyagin et al., 2019) and show that the previously estimated H₂O content in melts (3.9 ± 0.8 (2σ) wt %, Plank et al., 2013) are minimal. The results of this work on H₂O content in initial primitive magma of Eastern Volcanic belt of Kamchatka also confirm the idea of (Portnyagin et al., 2019) that most primitive island-arc inclusions did not preserve their initial H₂O content and that initial island-arc melts contain on average ≥ 4 wt % H₂O. This H₂O content in primary island-arc melts may imply the presence of a "crust filter" (Plank et al., 2009), as well as lower melting temperatures in the mantle and higher H₂O fluxes in subduction zones than was previously estimated based on direct determination of H₂O in potentially dehydrated melt inclusions.

This work was supported by RFBR project № 18-35-00529.

Experiments on partial homogenization of melt inclusions were supported by RFBR project 18-35-00497.

References

Almeev et al. The effect of H₂O on olivine crystallization in MORB: experimental calibration at 200 MPa // Am. Mineral., 2007, vol. 92, p. 670-674

The formation and differentiation of magmas

- Coogan et al. Aluminum-in-olivine thermometry of primitive basalts: evidence of an anomalously hot mantle source for large igneous provinces // *Chem. Geol.*, 2014, vol. 368, p. 1-10
- Danyushevsky et al. Re-equilibration of melt inclusions trapped by magnesian olivine phenocrysts from subduction-related magmas: petrological implications // *Contrib. to Min. and Petrol.*, 2000, №138, p. 68-83
- Ford et al. Olivine–liquid equilibria: temperature, pressure and composition dependence of the crystal/liquid cation partition coefficients for Mg, Fe²⁺, Ca, and Mn // *J. Petrol.*, 1983, vol. 24, p. 256-265
- Gaetani G. A. and Watson E. B. Open system behavior of olivine-hosted melt inclusions // *EPSL*, 2000, vol. 183, p. 27–41.
- Gaetani et al. Rapid re-equilibration of H₂O and oxygen fugacity in olivine hosted melt inclusions // *Geology*, 2012, vol. 40, p. 915-918
- Kamenetsky et al. Silicate-sulfide liquid immiscibility in modern arc basalt (Tolbachik volcano, Kamchatka): Part II. Composition, liquidus assemblage and fractionation of the silicate melt // *Chem. Geol.*, 2017, vol. 471, p. 92-110
- Krasheninnikov S.P. et al. Experimental Testing of Olivine–Melt Equilibrium Models at High Temperatures // *Doklady Earth Sciences*, 2017, vol. 475, Part 2, p. 919–922.
- Lange et al. The effect of H₂O, CO₂ and F on the density and viscosity of silicate melts, Volatiles in Magmas. *Rev. Mineral.*, Carrol, M.R. and Holloway, J.R., Eds., Washington: Mineral. Soc. Am., 1994, vol. 30, p. 331-369
- Mallmann, O'Neill. Calibration of an empirical thermometer and oxybarometer based on the partitioning of Sc, Y and V between olivine and silicate melt // *J. Petrol.*, 2013, vol. 54, № 5, p. 933-949
- Mironov et al. Quantification of the CO₂ budget and H₂O-CO₂ systematics in subduction-zone magmas through the experimental hydration of melt inclusions in olivine at high H₂O pressure // *EPSL*, 2015, vol. 415, p. 1-11
- Nazarova et al. Initial H₂O content and conditions of parent magma origin for Gorely Volcano (Southern Kamchatka) estimated by trace element thermobarometry // *Dokl. Earth Sci.*, 2017, vol. 472, № 3, p. 100-103.
- Plank et al. Why do mafic arc magmas contain ~4 wt % water on average? // *EPSL*, 2013, vol. 364, p. 168-179.
- Portnyagin et al. Constraints on mantle melting and composition and nature of slab components in volcanic arcs from volatiles (H₂O, S, Cl, F) and trace elements in melt inclusions from the Kamchatka arc // *EPSL*, 2007, vol. 255, № 1-2, p. 53-69.
- Portnyagin et al. Experimental evidence for rapid water exchange between melt inclusions in olivine and host magma // *EPSL*, 2008, vol. 272, p. 541-552.
- Portnyagin et al. Dehydration of melt inclusions in olivine and implications for the origin of silica under saturated island-arc melts // *EPSL*, 2019, vol. 517, P. 95-105.
- Shishkina et al. Solubility of H₂O- and CO₂-bearing fluids in tholeiitic basalts at pressures up to 500 MPa // *Chem. Geol.*, 2010, vol. 277, pp. 115-125.
- Sisson, Grove. Temperatures and H₂O contents of low MgO high alumina basalts // *Contrib. Mineral. Petrol.*, 1993, vol. 113, p. 167-184
- Sobolev, Chaussidon. H₂O concentrations in primary melts from island arcs and mid ocean ridges: implications for H₂O storage and recycling in the mantle // *EPSL*, 1996, vol. 137, p. 45-55.
- Sobolev et al. Komatiites reveal an Archean hydrous deep-mantle reservoir // *Nature*, 2016, vol. 531, № 7596, p. 628-632
- Sparks et al. Physical aspects of magmatic degassing. I. Experimental and theoretical constraints on visculation, Volatiles in Magmas. *Reviews in Mineralogy*, Carrol, M.R. and Holloway, J.R., Eds., Washington: Mineralogical Society of America, 1994, vol. 30, p. 413-445
- Tobelko et al. Compositions and Formation Conditions of Primitive Magmas of the Karymsky Volcanic Center, Kamchatka: Evidence from Melt Inclusions and Trace-Element Thermobarometry // *Petrology*, vol. 27, №3, p. 243-264
- Roedder. Fluid inclusions // *Miner. Soc. Amer., Michigan: Book Crafters Inc*, 1984, vol 12., p. 644